1432 *Biochemistry* **2011,** *50,* 1432–1441
DOI: 10.1021/bi1007589

BIOCHEMISTRY
including biophysical chemistry & molecular biology
Article

HU Binding to a DNA Four-Way Junction Probed by Förster Resonance Energy Transfer[†]

Codruta Iulia Vitoc and Ishita Mukerji*

Molecular Biology and Biochemistry Department, Molecular Biophysics Program, Wesleyan University, Middletown, Connecticut 06459-0175, United States

Received May 12, 2010; Revised Manuscript Received January 12, 2011

ABSTRACT: The *Escherichia coli* protein HU is a non-sequence-specific DNA-binding protein that interacts with DNA primarily through electrostatic interactions. In addition to nonspecific binding to linear DNA, HU has been shown to bind with nanomolar affinity to discontinuous DNA substrates, such as repair and recombination intermediates. This work specifically examines the HU−four-way junction (4WJ) interaction using fluorescence spectroscopic methods. The conformation of the junction in the presence of different counterions was investigated by Förster resonance energy transfer (FRET) measurements, which revealed an ion-type conformational dependence, where Na^+ yields the most stacked conformation followed by K^+ and Mg^{2+}. HU binding induces a greater degree of stacking in the Na^+-stabilized and Mg^{2+}-stabilized junctions but not the K^+-stabilized junction, which is attributed to differences in the size of the ionic radii and potential differences in ion binding sites. Interestingly, junction conformation modulates binding affinity, where HU exhibits the lowest affinity for the Mg^{2+}-stabilized form (24 μM^{-1}), which is the least stacked conformation. Protein binding to a mixed population of open and stacked forms of the junction leads to nearly complete formation of a protein-stabilized stacked-X junction. These results strongly support a model in which HU binds to and stabilizes the stacked-X conformation.

Protein-induced distortions of DNA structure such as kinking and bending have been recognized to play an important role in packaging DNA, processing stored DNA information, and regulating genomic function (*1*, *2*). The *Escherichia coli* histone-like protein HU[1] has been shown to be highly abundant in the cell and involved in nucleoid compaction (*2*−*4*). A DNA binding and bending protein, HU stabilizes DNA into bent conformations required for optimal assembly of higher-order protein−DNA complexes involved in replication, transcription, transposition, and DNA repair (*5*−*8*). This protein-induced distortion of DNA to facilitate the formation of functional complexes has led to the designation of HU as an architectural protein (*9*). Although HU promotes specific genomic and cellular events, it recognizes DNA without sequence specificity by primarily electrostatic interactions (*10*).

HU binds to noncanonical B-DNA structures such as nicked, gapped, and four-way junction (4WJ) DNA 50−100-fold tighter than to linear DNA (*11*−*17*). The nanomolar binding affinity observed for these distorted DNA structures suggests that HU may use a structure-based or indirect readout mechanism of recognition. The relatively high binding affinity for 4WJ DNA exhibited by HU has also been observed for other architectural proteins, such as high-mobility group (HMG) box proteins (*18*−*20*), H_1 and H_5 histones (*21*, *22*), and the SWI/SNF complex (*23*). Although the binding of endonucleases and resolvases to 4WJ DNA has been characterized by structure-based methods (*24*−*26*), less information is available regarding the structure and binding of junctions in complex with architectural proteins. In this study, the HU−4WJ interaction is studied to elucidate structural aspects of the interaction and illuminate function.

Cruciform or 4WJ DNA is the central DNA intermediate in homologous and site-specific recombination events (*27*, *28*). These structures, which can change conformation rapidly in solution, are also implicated in DNA repair and viral integration processes (*27*, *29*, *30*). A consensus view of Holliday junction structure has emerged from biophysical studies of immobilized DNA junctions, which are incapable of branch migration (*31*−*33*). In the absence of added metal ions, the junction exists in an open 4-fold symmetrical structure, with no central base stacking (*32*, *34*, *35*), which is capable of branch migration (*36*, *37*). In the presence of physiological concentrations of metal ions, 4WJ DNA becomes more compact by pairwise coaxial stacking of the helical arms, adopting a right-handed antiparallel stacked-X structure. Two stereochemically equivalent conformers of the antiparallel stacked-X structure can form depending upon the choice of stacking partners. In solution, both conformers are present in a dynamic equilibrium (Figure 1) (*33*, *38*−*41*). Bias for one conformer over the other has been observed to be dependent on base sequence and independent of ion concentration (*32*, *39*, *42*, *43*).

This study utilizes junction 3, previously characterized by Lilley and co-workers, as a nonmigrating model of a 4WJ (*31*). Steady-state and time-resolved energy transfer experiments (*35*, *44*) with a series of fluorescently labeled junction 3 molecules demonstrated

[†]This work was supported by grants from the National Science Foundation (MCB-0316625) and the Patrick and Catherine Weldon Donaghue Medical Research Foundation (DF00-118).

*To whom correspondence should be addressed. Phone: (860) 685-2422. Fax: (860) 685-2141. E-mail: imukerji@wesleyan.edu.

[1]Abbreviations: EMSA, electrophoretic mobility shift assay; FRET, Förster resonance energy transfer; 4WJ, four-way junction; HU, heat-unstable histone-like protein; RHO, tetramethylrhodamine; FAM, fluorescein; C_6, six-carbon linker; TAMRA, tetramethylrhodamine; TBE, Tris/borate/EDTA buffer; EDTA, *N*,*N*,*N*′,*N*′-ethylenediaminetetraacetic acid.

 Published on Web 01/14/2011

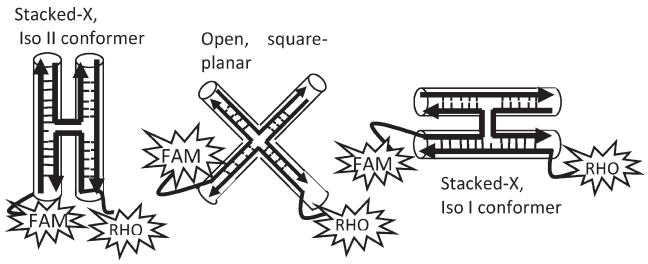

FIGURE 1: Schematic depiction of a four-way junction in the open-X form and the two stacked-X conformers, iso I and iso II. As shown, labeling of the R and X arms yields high FRET efficiencies for the iso II conformer.

that the junction adopts the stacked-X structure in the presence of metal ions and suggests that the predominant conformer results from the coaxial stacking of the B and X arms (iso II conformer) (Figure 1). These experiments were consistent with the gel electrophoretic migration patterns of the two junction conformations in the presence and absence of added metal ions (*32*). Structural dynamics of junction 3 have also been monitored using single-molecule fluorescence methodologies, which demonstrate that the junction is biased toward the iso II conformer in solution (77.4% vs 22.6%), and this conformer distribution is independent of ion concentration and temperature (*33*, *39*). The relative rates of conformer exchange ($k_{I\rightarrow II}$ = 12 s^{-1}, and $k_{II\rightarrow I}$ = 3.5 s^{-1}) indicate that the junction readily interchanges conformers. The overall structure of junction 3 has recently been determined by X-ray crystallography; the essential features of the junction as determined by solution-based methods were confirmed, including the observation of a 60° interduplex angle (*45*).

The FRET method has proven to be capable of deriving distance information over a broad range and has been used widely to monitor conformational changes in DNA induced by either protein or ion binding (*46*−*50*). This method has also been successfully applied in measuring the degree of distortion induced by the binding of HU (*51*) and the structurally identical but sequence-specific DNA-binding protein, integration host factor (*52*). In both cases, the equilibrium FRET measurements were consistent with bend angles determined by crystallography (*53*, *54*) and single-molecule methods (*55*), demonstrating the overall utility and accuracy of the method. In this study, we have employed Förster resonance energy transfer to study the ion-dependent conformational variations of Holliday junctions and the effects of HU binding. These measurements reveal that ion type in addition to concentration modulates junction conformation and further show that HU preferentially binds to and stabilizes the stacked-X conformation. In the presence of Na^+ and Mg^{2+}, protein binding leads to a more compact conformation, as measured by the distance between the arms of the junction.

EXPERIMENTAL PROCEDURES

HU Protein. HU protein was isolated and purified from *E. coli* strain RLM1078 (gift from R. McMacken), as previously described (*56*). Progressive enrichment of HU from the cell lysate was accomplished with three columns: SP-Sepharose column (Amersham-Pharmacia), DNA-cellulose column, and FPLC MonoS 5/5 or 10/10 cation exchange column (Amersham-Pharmacia). HU elutes at 0.4 M NaCl from the FPLC MonoS column. Because HU can co-elute with a nuclease, the lack of nuclease activity was verified by the absence of any digested products after incubation of the protein with plasmid DNA. Protein concentrations were calculated using the previously determined extinction coefficient ε_{230} of 37.5 mM^{-1} cm^{-1} (*56*).

Oligonucleotides. Oligonucleotides were purified using a 15% denaturing polyacrylamide gel (38:2) prepared in 7 M urea with 22.5 mM Tris base, 22.5 mM boric acid, and 0.625 mM Na_2EDTA (pH 8.3) (TBE). The gel was run under a constant voltage (300 V) at room temperature for 3 h. DNA bands were visualized and excised using UV shadowing and electroeluted (Schleicher and Schuell Elutrap, Concord, NH). Oligonucleotides were purchased from Integrated DNA Technologies (Coralville, IA): B, 5′-CCTCCGTCCTAGCAAGGGGCTGCTACCGGA-AGGG-3′; H, 5′-CCCTTCCGGTAGCAGCCTGAGCGGTG-GTTGAAGG-3′; R, 5′-CCTTCAACCACCGCTCAACTCA-ACTGCAGTCTGG-3′; X, 5′-CCAGACTGCAGTTGAGTC-CTTGCTAGGACGGAGG-3′.

Labeling of Oligonucleotides. X and R oligonucleotides were labeled at the 5′ end with single isomers: 5-carboxyfluorescein, succinimidyl ester (5-FAM, SE), and 5-carboxytetramethylrhodamine, succinimidyl ester (5-TAMRA, SE) (Molecular Probes, Eugene, OR) (*57*). The probes were covalently attached to the 5′ end of the oligonucleotide through an amino-modified six-carbon linker (C6). To obtain an accurate DNA concentration at 260 nm, we used a correction factor for the dye (*57*).

Assembly of Fluorescent Four-Way DNA Junctions. Fluorescent 4WJs with 17 bp arms used for FRET measurements were constructed via incubation of equal amounts of one fluorescein-labeled, X-strand, one rhodamine-labeled, R-strand, and two unlabeled strands in 10 mM Tris (pH 7.6), 300 mM NaCl, and 1 mM EDTA for 5 min at 80 °C, followed by slow cooling to room temperature in a water bath. Singly labeled junctions with rhodamine or fluorescein were prepared for control FRET, fluorescence anisotropy, and intensity measurements in the same manner. The four-stranded DNA structure was purified using a 6.5% native polyacrylamide gel (29:1) in TBE. The gel was run at 4 °C for 5−7 h at a constant voltage of 100 V. DNA was visualized and excised from the gel at a constant voltage of 100 V and 4 °C in TBE. Extracted cruciform DNA was dialyzed briefly against water and stored in a lyophilized form at −20 °C.

Fluorescence Measurements. Fluorescence intensity, anisotropy, and FRET measurements were performed in 10 mM Tris-HCl (pH 7.6) and 0.1 mM EDTA with either Na^+ or K^+ at the specified concentration. For experiments performed in the presence of Mg^{2+}, EDTA was not added to the solution. Measurements were performed using a Fluoromax-2 fluorometer (Horiba Jobin-Yvon, Edison, NJ) with a band-pass of 4 nm for excitation and 8 nm for emission. All experiments were performed at 10 °C, and the sample temperature was maintained with a circulating bath (RTE model 111, NESLAB Instruments, Inc.). Samples were stirred continuously in a 3 mm × 3 mm quartz cuvette (Starna Cell, Inc.). Fluorescein-labeled 4WJs were excited at 494 nm and monitored at 520 nm. Rhodamine-labeled 4WJs were excited at 555 nm, and emission was recorded at 585 nm. Reported values are from an average of six 5 s readings or averages of three scans from 510 to 630 nm at 1 nm/s. FRET measurements were performed with the polarizers set at 0° (excitation) and 55° (emission). Samples were excited at 490 nm, and the fluorescence intensity was monitored at 520 nm for the donor and 585 nm for the acceptor. For all titration experiments, the DNA concentration was held constant and either ions or HU was titrated into the solution. Protein binding affinity was measured under relatively high salt conditions (200 mM NaCl, 60 mM KCl, or 100 μM $MgCl_2$) or relatively low salt conditions (30 mM NaCl or 10 mM KCl).

Table 1: Equilibrium Binding Constants (K_a) Determined for HU−4WJ Interactions

ion concentration	stoichiometry	anisotropy (nM^{-1})	intensity (nM^{-1})	EMSA (nM^{-1})[a]
30 mM Na^+	2	0.35 ± 0.12[c] $K_1 = 2k = 0.70$[d] $K_2 = k/2 = 0.17$[d]	0.49 ± 0.17[e] $K_1 = 2k = 0.98$[d] $K_2 = k/2 = 0.24$[d]	not available
200 mM Na^+	2	0.19 ± 0.06[c] $K_1 = 2k = 0.38$[d] $K_2 = k/2 = 0.095$[d]	0.20 ± 0.07[e] $K_1 = 2k = 0.39$[d] $K_2 = k/2 = 0.10$[d]	0.022 ± 0.009[b]
10 mM K^+	2	0.20 ± 0.07[c] $K_1 = 2k = 0.39$[d] $K_2 = k/2 = 0.098$[d]	0.12 ± 0.04[e] $K_1 = 2k = 0.24$[d] $K_2 = k/2 = 0.06$[d]	not available
60 mM K^+	2	0.27 ± 0.09[c] $K_1 = 2k = 0.54$[d] $K_2 = k/2 = 0.13$[d]	0.30 ± 0.10[e] $K_1 = 2k = 0.60$[d] $K_2 = k/2 = 0.15$[d]	0.018 ± 0.006[b]
100 μM Mg^{2+}	2	0.024 ± 0.008[c] $K_1 = 2k = 0.048$[d] $K_2 = k/2 = 0.012$[d]	0.034 ± 0.011[e] $K_1 = 2k = 0.068$[d] $K_2 = k/2 = 0.017$[d]	0.024 ± 0.012[b]

[a]Electrophoretic mobility shift assay (data not shown). [b]K_{app}, apparent binding constant determined at 10 nM DNA. [c]Microscopic association constant. [d]Stepwise binding constant. [e]Determined from the fluorescence intensity change at 520 nm as a function of HU concentration.

Analysis of Binding. HU binding to 4WJ DNA was analyzed as previously described (*51*, *56*). Briefly, equilibrium binding curves were fit assuming identical, noninteracting binding sites:

$$i = i_0 + \frac{nk[\mathrm{L}](i_1 - i_0)}{1 + k[\mathrm{L}]}$$

where i, i_0, and i_1 represent the intensity of the titrated sample, free cruciform DNA, and cruciform DNA with one HU protein bound, respectively, L represents the free HU protein, k is the microscopic binding constant, and n is the number of bound HU dimers, determined from independent stoichiometry experiments. In these binding analyses, n was held constant at 2 and the fractional spectroscopic change was considered equal for each binding event. The anisotropy data were analyzed using a similar formulation in which anisotropy measurements replace intensity values.

FRET efficiency (E) as a function of ion concentration was fit to a two-state model for the folding of the junction:

$$E = E_0 + \frac{K_a[\mathrm{M}^+]^n(E_i - E_0)}{1 + K_a[\mathrm{M}^+]^n}$$

where E, E_i, and E_0 represent the FRET efficiency of the titrated sample and 4WJ DNA with and without ions, respectively, K_a is an apparent association constant for ion binding, and n is the Hill coefficient (*32*, *44*).

FRET Analysis. To determine R_0 values, quantum yields for the singly labeled donor 4WJ were measured relative to fluorescein in 0.1 M NaOH (*58*). The extinction coefficient used for the acceptor (rhodamine) was 84700 cm^{-1} M^{-1} (Invitrogen). Spectral calculations of the donor−acceptor overlap were performed using Grams AI (ThermoGalactic). We observe that the R_0 values are slightly affected by the concentration and type of ion in the solution (Table 1) and attribute these differences to dye−DNA interactions, which are influenced by ion concentration (*48*, *51*, *52*, *59*). Spectra used for calculating the spectral overlap and R_0 values were calculated in the presence of different ion types at the concentrations indicated for the experiments. Specifically, fluorescence and absorption data were obtained for the singly labeled junctions at the different ion concentrations used in the binding experiments. Thus, R_0 values were determined for each ion concentration at which distances are reported. The energy transfer efficiency (E) was calculated on the basis of the donor fluorescence decrease (*35*, *46*, *60*).

$$E = 1 - F_{DA}/F_D$$

The emission intensity at 520 nm, the wavelength of maximal donor emission, was measured for the donor alone (F_D) and for the donor in the presence of the acceptor (F_{DA}). The values of F_D and F_{DA} were normalized to donor concentrations and the relative amount of labeling (*46*, *60*). For all measurements with a single ion, F_D and F_{DA} values were obtained under the same conditions of ion concentration and type. For a quantitative comparison of the efficiencies obtained in the presence of different ions, the donor fluorescence intensities were ratioed against donor fluorescence obtained in an ion-free buffer (*61*). Efficiencies and distances were calculated considering the relative population of junctions in the iso II conformer as previously determined (*39*, *44*). The distance between donor and acceptor (R) was calculated using the following equation and the experimentally determined values for E and R_0 (*60*):

$$E = {R_0}^6/(R^6 + {R_0}^6)$$

Interduplex Angle Calculation. To determine the interduplex angle (IDA), we used the law of cosines, where the two junction arms and the distance between them are considered a triangle. The length of the junction arms was calculated assuming the helices have a canonical B-form geometry. Thus

$$c^2 = a^2 + b^2 - 2ab\cos\theta$$

where a, b, and c represent the lengths of the triangle sides, with side c opposite θ, the angle of interest or the interduplex angle. a and b are the lengths of the adjacent 4WJ arms (17 bp in length), and c is the distance separating the donor and the acceptor obtained by FRET.

RESULTS

Effect of Ions on 4WJ Conformation. To study the effect of *E. coli* HU binding on 4WJ structure, we initially characterized junction conformation in the presence of increasing concentrations of Mg^{2+}, K^+, and Na^+ ions. The choice of ion and the relative concentrations were determined in part by the binding

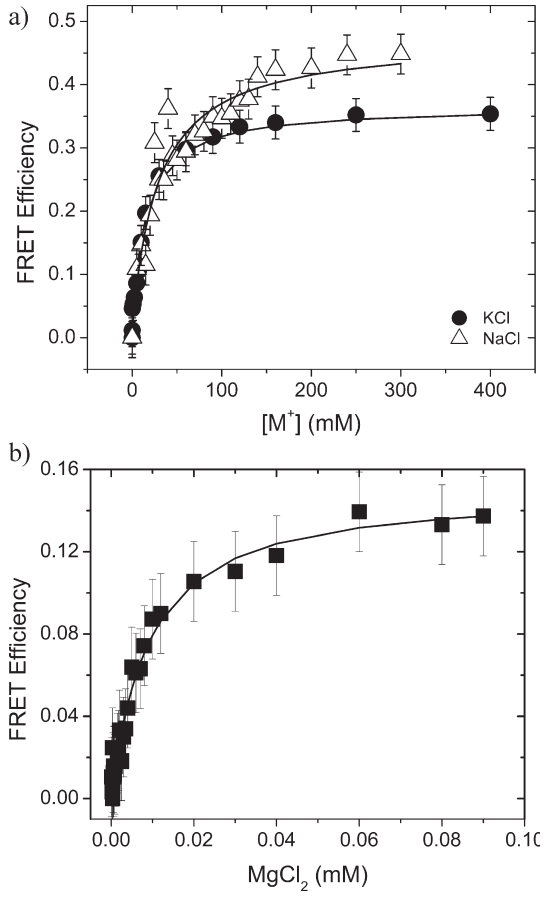

FIGURE 2: FRET efficiency change for the RX vector as a function of cation concentration: (a) Na^+ (△) and K^+ (●) and (b) Mg^{2+} (■). Data shown are fit to a two-state model of ion binding in which binding is relatively noncooperative giving a Hill coefficient n of 1.1 ± 0.1. The concentration of the 4WJ was 10 nM, and samples were contained in a continuously stirred 3 mm × 3 mm cuvette.

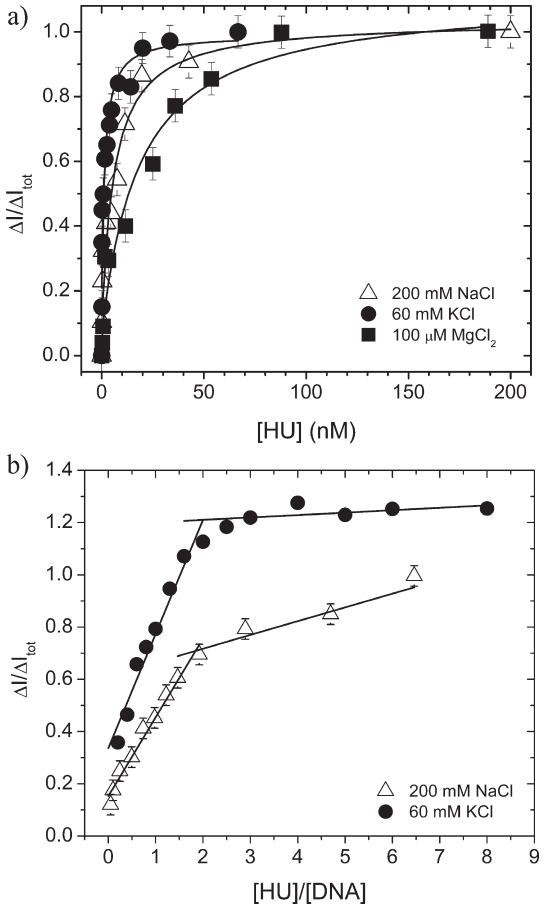

FIGURE 3: Determination of binding affinity and stoichiometry for HU bound to a 4WJ using fluorescence intensity. (a) Saturation binding of HU to 3 nM HJ measured with either 200 mM NaCl (△), 60 mM KCl (●), or 100 μM $MgCl_2$ (■). All experiments were conducted in 10 mM Tris buffer (pH 7.6) with the singly labeled fluorescein 4WJ using an excitation wavelength of 494 nm and monitoring emission at 520 nm. Equilibrium binding constants are listed in Table 1. (b) Stoichiometry of binding of HU to 4WJ DNA measured using fluorescence intensity. The intersection of the linear binding range with the plateau indicates the binding stoichiometry. Experiments were conducted at a constant DNA concentration of 50 nM. All experiments yield a stoichiometry of approximately two HU molecules to one 4WJ. Experimental conditions are the same as those described for panel a. Representative error bars are shown for the Na^+ data. The K^+ data are offset by a y-scale factor of 0.3 for the sake of clarity.

properties of the HU protein, as previously reported (*13*−*15*). The junction used for these experiments, junction 3, a stable, nonmigratable 4WJ, was originally developed and characterized by Lilley and co-workers (*31*). Previous characterization of the junction by FRET has shown that addition of Na^+, K^+, or Mg^{2+} leads to the coaxial stacking of the 17 bp junction arms to form a quasi-continuous helix and an increase in FRET efficiency (*32*, *35*, *44*) (Figure 1). To fully characterize the effect of HU binding in these different ion environments, FRET measurements were performed as a function of ionic strength and were used to determine the relative ion concentrations needed to induce the stacked-X conformation of the junction (Figure 2). These measurements were performed by labeling the X and R junction arms at the 5′ ends with fluorescein and rhodamine, respectively, using a C6 amino linker. The X and R arms were chosen for labeling because previous work had shown that labeling of these arms gives the largest change in FRET efficiency upon adoption of the stacked conformation (*35*, *46*, *62*).

As shown in Figure 2, the FRET efficiency increases with ion binding and plateaus upon saturation. Efficiency values at low concentrations of ions are less than 0.05; these low transfer efficiencies are consistent with a high concentration of open or square planar junctions. Addition of ions leads to an overall efficiency change that was largest for the Na^+-stabilized junction (Na^+-4WJ) (ΔE = 0.4) and smallest for the Mg^{2+}-stabilized junction (Mg^{2+}-4WJ) (ΔE = 0.12). The efficiency change is correlated with the increasing proximity of the X and R arms that form the stacked-X junction, and the larger efficiency change of the Na^+-4WJ is indicative of a shorter distance between the X and R arms and, consequently, a smaller interduplex angle relative to the Mg^{2+}-4WJ. The K^+-stabilized junction yields a moderate change in transfer efficiency (ΔE = 0.3) consistent with a smaller distortion relative to Na^+, but greater than that with Mg^{2+}. Because the junction can adopt either the iso I or the iso II conformer in the stacked form, the relative populations of junctions in the iso II conformer were assumed to be the same as those previously determined by single-molecule fluorescence and equilibrium FRET methods (*33*, *39*, *44*). In those studies, it was observed that the iso II population for junction 3 was approximately 77% in Na^+ and Mg^{2+} (*33*, *39*, *44*), and this population distribution is relatively constant over the ion concentrations employed. In our analyses, we have assumed that in

Table 2: FRET Determination of Distances and the Corresponding Interduplex Angles (IDA)

	without HU				with HU			
ion concentration and type	efficiency	R (Å)	interduplex angle (deg)[a]	R_0 (Å)	efficiency	R (Å)	interduplex angle (deg)[a]	R_0 (Å)
30 mM NaCl	0.28 ± 0.05	63.3 ± 2.8		52.5 ± 4.2	0.66 ± 0.04	48.2 ± 1.4	42.2 ± 1.4	53.8 ± 4.2
200 mM NaCl	0.42 ± 0.05	48.4 ± 1.6	42.5 ± 1.6	45.8 ± 3.7	0.64 ± 0.03	43.8 ± 1.4	37.9 ± 0.9	48.3 ± 3.7
10 mM KCl	0.16 ± 0.02	70.3 ± 1.7		53.3 ± 4.2	0.31 ± 0.01	63.3 ± 0.5	57.6 ± 0.5	52.6 ± 4.2
60 mM KCl	0.35 ± 0.05	58.7 ± 2.2	52.8 ± 2.2	52.9 ± 4.2	0.32 ± 0.02	62.2 ± 1.0	56.4 ± 1.0	54.8 ± 4.2
100 μM $MgCl_2$	0.15 ± 0.01	66.4 ± 1.2	60.8 ± 1.2	49.7 ± 4	0.27 ± 0.05	59.6 ± 2.5	53.7 ± 2.6	50.5 ± 4

[a]Interduplex angles were determined with the law of cosines using a junction arm length of 17 bp (17 bp × 3.4 Å) with the addition of linker length L to the arm labeled with fluorescein, where the linker has a full length (L) of 13.5 Å (*72*). For rhodamine, it is assumed that the dye stacks on the end of the DNA; therefore, the linker length is set to 0. FRET efficiencies are measured between X and R arms and are based on three independent measurements. The macroscopic IDA is defined as the angle from the end of a stacked arm to the center of the junction and to end of the opposite arm (*43*).

the presence of K^+ the same distribution of conformer populations is observed (77% iso II) based on the observation that the conformer distribution depends in part on the free energy of coaxial helix stacking, which is determined by sequence of the junction (*44*) as well as the fact that mobility patterns in gel experiments indicate that K^+ stabilizes the iso II conformer (*32*). Thus, if the conformer distribution is slightly altered in K^+, this would introduce some error into our calculation of absolute transfer efficiencies and bend angles; however, the relative changes as induced by protein binding are not affected.

The relative amount of metal ion needed to induce a change in junction conformation was assessed using a two-state binding model. The two states considered were the ion-free open state and the ion-induced stacked-X structure. Because the ion-binding site is not well-defined, an apparent dissociation constant was defined as the concentration at which 50% of the junction is in the stacked or open form. These analyses yielded apparent K_d values of 29 ± 4 and 5−6 mM for Na^+ and K^+, respectively, and Hill coefficients of approximately 1. As shown in Figure 2, Mg^{2+} achieves a 50% population of the stacked conformation at 4 ± 2 μM and is most effective at changing junction structure as a function of concentration. For Mg^{2+}, ion binding was also found to be relatively noncooperative, consistent with earlier observations (*31*, *39*, *44*). Although Mg^{2+} changes the junction structure at the lowest concentration of the ions monitored, the relative amount of ion-induced distortion of the structure is the least based on FRET measurements (Figure 2b). The junction is fully folded by 80−100 μM $MgCl_2$, which is consistent with previous results as determined in the gel (*32*). These apparent K_d values are lower than those previously reported for junction 1 (154 mM NaCl and 120 μM $MgCl_2$) (*44*); however, we note that junction 1 is biased toward the iso I conformer and has a different sequence at the junction. Therefore, the lower ion affinity observed for junction 1, which is 5- and 30-fold lower for Na^+ and Mg^{2+}, respectively, probably results from the differences in sequence at the junction and conformer bias.

Binding Affinity of the HU−4WJ Interaction. To probe the nature of the observed increased binding affinity of HU for 4WJ DNA, we monitored formation of the HU−4WJ complex by fluorescence anisotropy and intensity (Figure 3). Binding measurements were performed with a constant concentration of singly labeled 4WJ DNA (3 nM), and the affinity as measured by either method was the same within error (Table 1). HU binding affinity was measured under high-ionic strength conditions where the junction is in the stacked-X conformation, specifically 200 mM NaCl, 60 mM KCl, or 100 μM $MgCl_2$. For all three ions examined, protein binding leads to a change in fluorescence intensity, which plateaus at protein concentrations higher than 20 nM. The magnitude of the change in intensity is approximately 15−30% for the different ion−junction complexes examined. Analysis of the binding data was done assuming two identical noninteracting binding sites with little to no cooperativity (vide infra). These analyses yielded good fits to the data as shown (Figure 3), and therefore, more complicated binding functions were not invoked. We report microscopic association constants that can be related to the stepwise binding constants, such that $K_1 = 2k$ and $K_2 = k/2$ (Table 1). These analyses yield binding constants ranging from 0.19 to 0.30 nM^{-1} in the presence of Na^+ or K^+, consistent with previously reported values as determined by EMSAs (Table 2) (*12*−*15*). The weakest relative binding affinity (0.024−0.034 nM^{-1}) was measured in the presence of Mg^{2+} (Table 1).

The relative affinity of HU for labeled or unlabeled 4WJ DNA was also measured by EMSAs, which yielded apparent binding constants that were lower than those measured in solution potentially because of the higher concentration of 4WJ DNA used (10 nM), rapid dissociation of the complexes, and dilution effects in the gel (Table 1). At the higher DNA concentrations used for EMSAs, the analyses are also complicated by nonspecific HU binding that leads to an apparent weaker overall binding constant. In this study, EMSA measurements were used to ensure that the dye does not interfere with the HU binding interaction, and no appreciable differences were detected between the labeled and unlabeled 4WJ DNA.

The stoichiometry of HU binding to cruciform DNA was determined by monitoring the changes in fluorescence intensity using a 4WJ concentration that is 8−10-fold greater than the dissociation constant. Under these conditions, any HU protein introduced into the solution binds to the 4WJ. Once all of the binding sites have been saturated, it is expected that no further change in the fluorescence intensity will be observed. For the Na^+- and K^+-stabilized junctions, a pronounced discontinuity in the binding function is observed at a HU:4WJ mole ratio of approximately 2:1 (Figure 3). In these measurements of binding stoichiometry, an intensity increase is observed in the plateau regions, which is attributed to some nonspecific binding at higher concentrations of HU and is more pronounced for Na^+. FRET measurements demonstrate, however, that the conformational change induced by HU binding occurs at a mole ratio of 2:1 and is not caused by nonspecific, low-affinity binding of the protein (Figure 5). Thus, in all analyses of the HU−4WJ binding interaction, the stoichiometry of binding was held constant at two HU dimers to one 4WJ.

To further probe the nature of the HU−4WJ interaction and address whether HU binding affinity is dependent on junction conformation, we measured binding affinity under conditions of

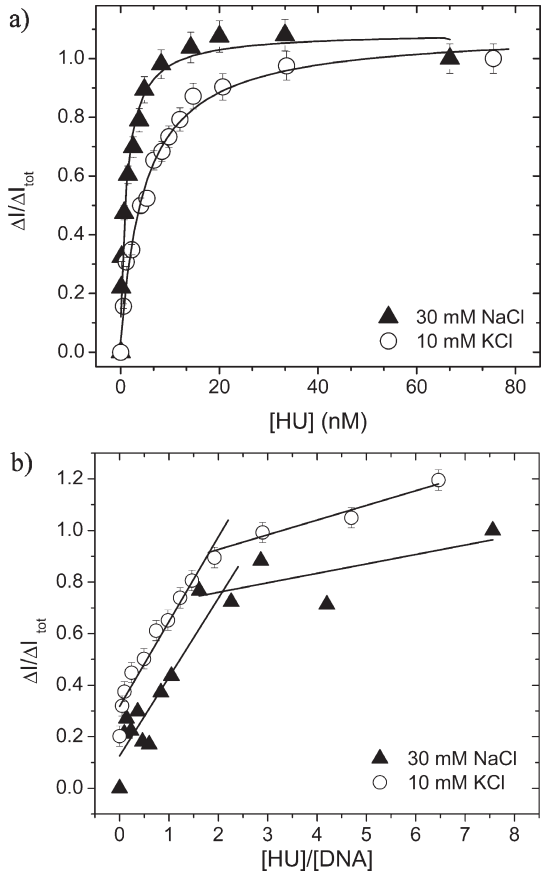

FIGURE 4: HU binding characteristics under low-ionic strength conditions determined by fluorescence intensity. (a) Saturation binding of HU to 3 nM HJ measured at 30 mM NaCl (▲) and 10 mM KCl (○). Equilibrium binding constants are listed in Table 1. (b) Stoichiometry of binding of HU to 4WJ DNA determined using fluorescence intensity. The intersection of the linear binding range with the plateau indicates the binding stoichiometry. These experiments yield a stoichiometry of approximately two HU molecules to one 4WJ and were conducted at a constant DNA concentration of 50 nM. Binding and stoichiometry experiments were performed on a singly labeled fluorescein 4WJ in 10 mM Tris buffer (pH 7.6) using an excitation wavelength of 494 nm and monitoring emission at 520 nm. Representative error bars are shown for the KCl data, which are offset by a *y*-scale factor of 0.2 for the sake of clarity.

relatively low ionic strength, 30 mM NaCl or 10 mM KCl (Figure 4a). These conditions allowed us to probe HU binding affinity in the presence of both open and closed forms of the 4WJs. The experiments could not be performed with the junction completely in the open conformation, because the protein was not stable in the absence of cations. At these salt concentrations, as shown in Figure 2, approximately 50% or more of the junction molecules adopt the stacked-X conformation. Stoichiometric HU binding leads to a relatively steep increase in either fluorescence intensity or anisotropy, which plateaus at a protein concentration that is approximately double that of the DNA consistent with a 2:1 HU:4WJ ratio. At higher protein:4WJ ratios, an increase in intensity is observed, which is attributed to nonspecific binding of HU to the 4WJ (Figures 3b and 4b). Nonspecific binding of HU to the arms of the junctions was also previously detected in EMSA experiments (*13*−*15*). Binding curves, measured by either anisotropy or fluorescence intensity at low ionic strengths, were described well by a model of identical and noninteracting binding sites, in which the number of binding sites was kept constant at two (Figure 4a). Under these conditions,

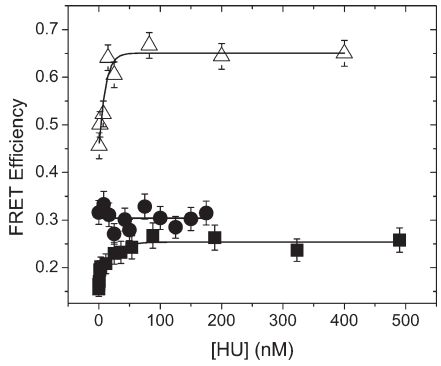

FIGURE 5: Energy transfer efficiency change (*E*) as a function of HU concentration. In all experiments, 10 nM doubly labeled junction was incubated with HU under high-salt conditions: 200 mM NaCl (△), 60 mM KCl (●), and 100 μM $MgCl_2$ (■). The curves are shown as a visual aid only and do not correspond to a binding curve because of the DNA concentration used. Buffer conditions are the same as those described in the legend of Figure 3.

the equilibrium HU binding affinities were found to be approximately 0.49 and 0.12 nM^{-1} for the Na^+-4WJ and K^+-4WJ, respectively (Table 1), which is the same within error as that observed at 200 mM Na^+ and 60 mM K^+. Thus, within this relatively narrow range of ion concentrations, the binding affinity of HU for the 4WJ remains relatively constant (Table 1).

Modulation of 4WJ Conformation by HU. The global structure of the complex formed between HU and the 4WJ was investigated using steady-state FRET measurements. For Na^+- and Mg^{2+}-stabilized junctions, protein binding leads to an increase in FRET efficiency, consistent with a reduction in the distance between the arms and a stacked junction conformation (Figure 5). In the presence of 200 mM Na^+, a final efficiency of 0.64 was observed, while for 100 μM Mg^{2+}, the final FRET efficiency was 0.27. The FRET efficiency was dependent on protein concentration and saturable for Na^+ and Mg^{2+} and was correlated with the K_a as measured by intensity and anisotropy, confirming that the change in FRET efficiency was associated with protein binding. The degree of stacking, as measured by efficiency, increased by approximately 14% as a result of HU binding in the presence of Mg^{2+} or Na^+.

Interestingly, HU binding in the presence of 60 mM K^+ did not lead to a significant change in FRET efficiency (Figure 5), suggesting that protein binding under these conditions does not change the structure of the K^+-stabilized junction. From these FRET measurements, we infer that in these comparisons the 4WJ structure adopts the most stacked conformation in the presence of Na^+ and HU. In the presence of K^+, the population of junctions in the iso II conformer is assumed to be 80% based on gel experiments (*32*). If the conformer distribution were significantly different, then the degree of stacking would be greater with K^+ and more similar to that with Na^+; however, this type of distribution is not supported by the gel experiments. Interestingly, the HU−K^+-stabilized junction complex exhibits the largest interduplex angle (IDA) in this investigation.

Protein-induced conformational changes of the 4WJ were also monitored by FRET in the presence of either 30 mM NaCl or 10 mM KCl. From our ion titrations shown in Figure 2, it is expected that under these conditions approximately 50% or more of the junctions are in the stacked-X conformations. As expected, FRET efficiencies at the starting point of these titrations are approximately 0.16 (10 mM KCl) or 0.32 (30 mM NaCl), approximately half of the efficiency observed at 60 mM KCl or 200 mM

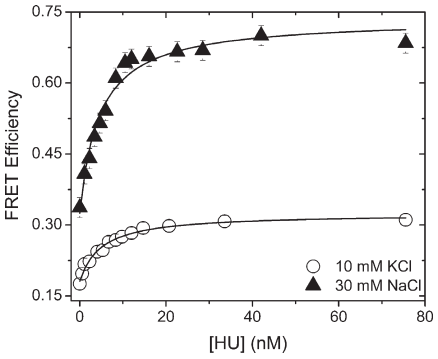

FIGURE 6: Energy transfer efficiency change (*E*) as a function of HU concentration. In all experiments, 10 nM doubly labeled junction was incubated with HU under low-salt conditions: 30 mM NaCl (▲) and 10 mM KCl (○). The curves are shown as a visual aid only and do not correspond to a binding curve because of the DNA concentration used. Buffer conditions are the same as those described in the legend of Figure 3.

NaCl, consistent with a 50% population of stacked junctions (Figure 6). Binding of HU to the cruciform leads to an increase in FRET efficiency, which reaches maximal values of 0.32 and 0.64 for K^+ and Na^+, respectively (Figure 6). These values were similar to the ones determined at 60 mM KCl and 200 mM NaCl for the HU_2−4WJ interactions (Figure 5) and suggest that at these different concentrations of KCl and NaCl, HU binding induces a similar stacked-X junction structure.

The observation of the same FRET efficiencies and binding stoichiometries at low and high concentrations of NaCl and KCl under saturating binding conditions provides strong evidence that HU binding shifts the equilibrium completely to the stacked form. If some junctions were still in the open form, the FRET efficiency would be lower than that measured with 100% of the junctions in the stacked form (i.e., at high salt concentrations), because the measured value is a weighted average of all species in solution. The starting efficiency of the titration at low concentrations of ions confirms that the FRET values result from consideration of a weighted average of open and stacked forms. Thus, our data indicate that HU binding drives the equilibrium to the most stacked form and is suggestive that HU binding essentially locks the 4WJ into the stacked-X conformation. The affinity of HU for the Mg^{2+}−4WJ complex is approximately 8−10-fold weaker than for the Na^+-4WJ complex, suggesting that HU binding affinity for the open junction is lower than that for the stacked junction. However, we cannot rule out the possibility that the modestly weaker binding affinity results because of the increased charge density of the Mg^{2+} ions.

DISCUSSION

Junction Angle and the Role of Ions. We have investigated the structure of junction 3, a nonmigratable 4WJ, in the presence of relatively low and high concentrations of Na^+, K^+, and Mg^{2+} and monitored the effects of HU binding. Under these conditions, we find that the structure of the 4WJ in the absence of protein is dependent not only on the ionic strength of the solution as expected (*32*, *62*) but also on ion type.

FRET determination of the structure is influenced by several factors, most notably the fluorescent dyes. Because the dyes are tethered to the 4WJ by a six-carbon linker at the 5′ end with conformational flexibility, their positions are not well-defined. Several lines of evidence indicate that rhodamine stacks with the DNA and adopts multiple conformations when attached to DNA (*48*, *51*, *52*, *63*) similar to what has been observed for the Cy3 and Cy5 dyes (*59*); therefore, we have primarily considered the length of one linker, that attached to the fluorescein, in determining the angle of the junction. Because the junction arms are relatively long (17 bp) and equivalent, the junction angle of this construct is considered to be independent of the length of the arms (*43*); thus, the position of the linker should not have a significant affect on the IDA (Table 2). In previous measurements, the conformation of junction 3 was mainly investigated in the presence of Mg^{2+} and the angle for the stacked conformation was approximately 60° (*62*). A recent X-ray crystal structure of junction 3 has confirmed that the IDA is approximately 60° and also confirmed other details of junction architecture determined by FRET (*45*). The angle, determined in the presence of Mg^{2+} from the current FRET efficiency measurements, is approximately 61° and is consistent with those measured in previous studies (*45*, *62*) and by single-molecule methods (*64*).

We observe that the IDAs determined for the Na^+-4WJ with and without HU are 38° and 42°, respectively, and that the Na^+-4WJ is the most compact of the ions examined. We do not report IDA values for the junctions stabilized by 30 mM Na^+ and 10 mM K^+ in the absence of HU because of the heterogeneous nature of those populations. We note that the 30 mM Na^+-stabilized 4WJ in the presence of saturating amounts of HU yields a longer distance and consequently greater IDA relative to that of the 200 mM Na^+-stabilized HU-bound 4WJ. Although these differences are outside our range of error, they are considerably smaller than the changes observed for junctions without HU or stabilized by a different ion. Nevertheless, our findings are consistent with previous studies in which high concentrations of Na^+ were needed to induce the most stacked form of the junction (*32*, *44*).

Folding of the junction into the compact X- structure involves the placement of the exchanging phosphate groups approximately 6.2 Å apart at the strand exchange point (*65*, *66*), leading to significant electrostatic repulsion. The introduction of methyl phosphonates to reduce this electrostatic repulsion influences the folding of the junction, demonstrating the importance of charge neutralization in the stacked form (*32*). X-ray crystal structure determinations of Holliday junctions have detected a Na^+ ion in the center of the junction at the region of highest electronegativity (*65*, *66*), and ions were observed in the same general area in other structures (*67*), suggestive that in solution the affinity for ions in this region is significant. Uranyl photocleavage experiments also indicate that this is a likely site for ion binding (*68*).

It is not expected that ions bind site-specifically to the junction; however, a relatively high concentration of positive charge is needed to screen the electrostatic repulsion of the phosphates and fold the junction, and this concentration is higher for monovalent ions than for divalent ions. The positive charge density, provided by the ions, is relatively mobile, although it is likely that the ion residence time in the center of the junction is longer than along the arms of the junction.

The X-ray crystal structures with ions present reveal that the ions are hydrated and interaction with the DNA may be mediated through solvent molecules (*67*); therefore, the degree of junction distortion upon binding K^+ and Mg^{2+} may be determined in part by the hydrated radius of the ion (2.7 and 2.1 Å, respectively) (*69*) and the energetically unfavorable cost of dehydrating the ion to coordinate to the phosphate backbone. Our results suggest that the electronegative cleft at the center of the junction is occupied to

a different extent on the basis of the ion concentration, ionic radius, and degree of hydration, and we speculate that the size of the hydrated ion determines in part the degree of junction distortion. Consistent with this idea, K^+, which has the larger hydrated radius, stabilizes the most open form of the junction in the presence of HU with an IDA of 57° (Table 2).

Protein-Induced Junction Conformation. Overall, fluorescent measurements investigating the binding of HU to the 4WJ have revealed that two HU dimers bind to one junction with nanomolar binding affinity, stabilize the stacked-X conformation, and in the presence of Na^+ and Mg^{2+} induce a more distorted structure. Affinity measurements are in good agreement with those previously determined in the gel by Rouvière-Yaniv and co-workers (*12*−*14*). Although the junction can exist in two stacked conformer configurations, the FRET measurements report only on the presence of the iso II conformer because of the position of the labels (Figure 1). Junction 3, used in this study, is biased toward the iso II conformer, and previous bulk and single molecule fluorescence studies, suggested that the relative distribution of conformers is determined mainly by sequence and not ion concentration (*39*, *46*). Detection of conformers in the gel in the presence of Na^+ and K^+ has also indicated that junction 3 is strongly biased toward the iso II conformer (*32*). Previous gel studies of binding of HU to junction 3 in the presence of Na^+ also support a predominately iso II conformation for the protein-bound form with approximately 20% iso I (*13*). Thus, for all the ions investigated, we have assumed that approximately 77% of the junction 3 molecules adopt the iso II conformer as previously determined in single-molecule studies (*39*). We note that differences in the conformer population would affect the absolute transfer efficiencies determined and, consequently, the angles reported, but the relative change in efficiency as a consequence of protein binding would be unaffected.

Current results indicate that at low concentrations of Na^+ and K^+ with saturating amounts of bound HU, the bulk of the junctions are in the stacked-X form. This suggests that HU binding perturbs the equilibrium between the open and stacked forms of the junction, resulting in mainly stacked junctions. Single-molecule experiments have demonstrated that the junctions are dynamic structures rapidly sampling open and stacked conformations (*33*, *39*). We suggest that HU perturbs the equilibrium between these forms by binding to the stacked form and reducing the concentration of protein-free junctions in the stacked conformation. Re-establishment of equilibrium in the context of HU binding reduces the overall number of junctions in the open, square planar conformation. Under saturating binding conditions, the observation of junctions primarily in the stacked form when starting from equal populations of stacked and open junctions can be explained by two possibilities. (1) The protein binds to the stacked-X conformation and captures it as in the high-salt case, or (2) the protein binds to the open conformation and distorts the junction into the stacked-X structure. The equilibrium nature of our study prevents a direct elucidation of these mechanisms.

Several cocrystal structures of proteins bound to a 4WJ in which protein binding leads to a distortion of the junction into a more open conformation have been obtained, contrary to what is observed with HU (*24*, *26*, *62*). The HU functional analogue in eukaryotes, HMG, also binds to 4WJs with high affinity; however, in marked contrast to HU, HMG recognizes only the open form of the junction (*19*). Although protein−junction structures differ in the degree of distortion induced by protein binding, some amount of opening at the junction point is consistently observed (*24*), and despite the relatively small IDA observed, we cannot rule out the possibility that some opening in the central region is occurring in the HU−4WJ complex. The IDA values of ~40° in the T4 endonuclease VII−4WJ complex are similar to that detected for HU binding to the Na^+-4WJ, and T4 endonuclease VII binding leads to an opening of the junction central region (*70*). Other proteins such as hMSH4-hMSH5 and Brca1 similarly bind 4WJs with nanomolar affinity and are thought to stabilize the stacked-X form (*30*, *71*). This stabilization may be functionally related to a suppression of recombination, and it is tempting to speculate that HU may play a similar role in *E. coli* because the relatively high cellular concentrations of HU observed predict that it will be bound to any cruciform structures present (*3*). Further investigation of the structure of different protein−4WJ complexes may help to elucidate the possible functions.

ACKNOWLEDGMENT

We thank Prof. Roger McMacken for the gift of the RLM 1078 *E. coli* strain, Prof. Manju Hingorani for her technical assistance and helpful discussions, Kristi Wojtuszewski for technical training, and Andrew Moreno and Soumya Ramananda for help in protein preparation.

REFERENCES

1. Werner, M. H., Gronenborn, A. M., and Clore, G. M. (1996) Intercalation, DNA kinking, and the Control of Transcription. *Science 271*, 778–784.
2. Drlica, K., and Rouviere-Yaniv, J. (1987) Histonelike Proteins of Bacteria. *Microbiol. Rev. 51*, 301–319.
3. Azam, T. A., and Ishihama, A. (1999) Twelve species of the Nucleoid-associated Protein from *Escherichia coli*. *J. Biol. Chem. 274*, 33105–33113.
4. Kar, S., Edgar, R., and Adhya, S. (2005) Nucleoid remodeling by an altered HU protein: Reorganization of the transcription program. *Proc. Natl. Acad. Sci. U.S.A. 102*, 16397–16402.
5. Dixon, N. E., and Kornberg, A. (1984) Protein HU in the enzymatic replication of the chromosomal origin of *Escherichia coli*. *Proc. Natl. Acad. Sci. U.S.A. 81*, 424–428.
6. Boubrik, F., and Rouviere-Yaniv, J. (1995) Increased sensitivity to γ irradiation in bacteria lacking protein HU. *Proc. Natl. Acad. Sci. U.S.A. 92*, 3958–3962.
7. Aki, T., and Adhya, S. (1997) Repressor induced site-specific binding of HU for transcriptional regulation. *EMBO J. 16*, 3666–3674.
8. Lavoie, B. D., Shaw, G. S., Millner, A., and Chaconas, G. (1996) Anatomy of a Flexer-DNA Complex inside a Higher-Order Transposition Intermediate. *Cell 85*, 761–771.
9. Travers, A. (1993) DNA-Protein Interactions: The three-dimensional architecture of DNA-protein complexes. In DNA-Protein Interactions, pp 28−51, Chapman & Hall, London.
10. Swinger, K. K., and Rice, P. A. (2004) IHF and HU: Flexible architects of bent DNA. *Curr. Opin. Struct. Biol. 14*, 28–35.
11. Castaing, B., Zelwer, C., Laval, J., and Boiteux, S. (1995) HU Protein of *Escherichia coli* Binds Specifically to DNA That Contains Single-strand Breaks or Gaps. *J. Biol. Chem. 270*, 10291–10296.
12. Pinson, V., Takahashi, M., and Rouviere-Yaniv, J. (1999) Differential Binding of the *Escherichia coli* HU, Homodimeric Forms and Heterodimeric Form to Linear, Gapped and Cruciform DNA. *J. Mol. Biol. 287*, 485–497.
13. Kamashev, D., Baladina, A., and Rouviere-Yaniv, J. (1999) The binding motif recognized by HU on both nicked and cruciform DNA. *EMBO J. 18*, 5434–5444.
14. Bonnefoy, E., Takahashi, M, and Yaniv, J. R. (1994) DNA-binding Parameters of the HU Protein of *Escherichia coli* to cruciform DNA. *J. Mol. Biol. 242*, 116–129.
15. Kamashev, D., and Rouviere-Yaniv , J. (2000) The histone-like protein HU binds specifically to DNA recombination and repair intermediates. *EMBO J. 19*, 6527–6535.
16. Swinger, K. K., and Rice, P. A. (2007) Structure-based analysis of HU-DNA binding. *J. Mol. Biol. 365*, 1005–1016.

17. Ghosh, S., and Grove, A. (2006) The *Deinococcus radiodurans*-encoded HU protein has two DNA-binding domains. *Biochemistry 45*, 1723–1733.
18. Bianchi, M. E., Beltrame, M., and Paonessa, G. (1989) Specific recognition of cruciform DNA by nuclear protein HMG1. *Science 243*, 1056–1059.
19. Pöhler, J. R. G., Norman, D. G., Bramham, J., Bianchi, M. E., and Lilley, D. M. J. (1998) HMG box proteins bind to four-way DNA junctions in their open conformation. *EMBO J. 17*, 817–826.
20. Zlatanova, J., and Holde, K. V. (1998) Binding to four-way junction DNA: A common property of architectural proteins? *FASEB J. 12*, 421–431.
21. Varga-Weisz, P., van Holde, K., and Zlatanova, J. (1994) Competition between linker histones and HMG1 for binding to four-way junction DNA: Implications for transcription. *Biochem. Biophys. Res. Commun. 203*, 1904–1911.
22. Varga-Weisz, P., van Holde, K., and Zlatanova, J. (1993) Preferential binding of histone H1 to four-way helical junction DNA. *J. Biol. Chem. 268*, 20699–20700.
23. Quinn, J., Fyrberg, A. M., Ganster, R. W., Schmidt, M. C., and Peterson, C. L. (1996) DNA-binding properties of the yeast SWI/SNF complex. *Nature 379*, 844–847.
24. Declais, A. C., and Lilley, D. M. (2008) New insight into the recognition of branched DNA structure by junction-resolving enzymes. *Curr. Opin. Struct. Biol. 18*, 86–95.
25. Lilley, D. M., and White, M. F. (2001) The junction-resolving enzymes. *Nat. Rev. Mol. Cell Biol. 2*, 433–443.
26. Khuu, P. A., Voth, A. R., Hays, F. A., and Ho, P. S. (2006) The stacked-X DNA Holliday junction and protein recognition. *J. Mol. Recognit. 19*, 234–242.
27. Holliday, R. (1964) A mechanism for gene conversion in fungi. *Genet. Res. 5*, 282–304.
28. Liu, Y., and West, S. C. (2004) Happy Hollidays: 40th anniversary of the Holliday junction. *Nat. Rev. Mol. Cell Biol. 5*, 937–944.
29. Marsischky, G. T., Lee, S., Griffith, J., and Kolodner, R. D. (1999) *Saccharomyces cerevisiae* MSH2/6 complex interacts with Holliday junctions and facilitates their cleavage by phage resolution enzymes. *J. Biol. Chem. 274*, 7200–7206.
30. Snowden, T., Acharya, S., Butz, C., Berardini, M., and Fishel, R. (2004) hMSH4-hMSH5 Recognizes Holliday Junctions and Forms a Meiosis-Specific Sliding clamp that Embraces Homologous Chromosomes. *Mol. Cell 15*, 437–451.
31. Duckett, D. R., Murchie, A. I., Diekmann, S., von Kitzing, E., Kemper, B., and Lilley, D. M. (1988) The structure of the Holliday junction, and its resolution. *Cell 55*, 79–89.
32. Duckett, D. R., Murchie, A. I., and Lilley, D. M. (1990) The role of metal ions in the conformation of the four-way DNA junction. *EMBO J. 9*, 583–590.
33. McKinney, S. A., Declais, A. C., Lilley, D. M., and Ha, T. (2003) Structural dynamics of individual Holliday junctions. *Nat. Struct. Biol. 10*, 93–97.
34. Liu, J., Declais, A. C., and Lilley, D. M. (2004) Electrostatic interactions and the folding of the four-way DNA junction: Analysis by selective methyl phosphonate substitution. *J. Mol. Biol. 343*, 851–864.
35. Clegg, R. M., Murchie, A. I., and Lilley, D. M. (1994) The solution structure of the four-way DNA junction at low-salt conditions: A fluorescence resonance energy transfer analysis. *Biophys. J. 66*, 99–109.
36. Panyutin, I. G., Biswas, I., and Hsieh, P. (1995) A pivotal role for the structure of the Holliday junction in DNA branch migration. *EMBO J. 14*, 1819–1826.
37. Panyutin, I. G., and Hsieh, P. (1994) The kinetics of spontaneous DNA branch migration. *Proc. Natl. Acad. Sci. U.S.A. 91*, 2021–2025.
38. Graiger, R. J., Murchie, A. I. H., and Lilley, D. M. J. (1998) Exchange between Stacking Conformers in a Four-Way Junction. *Biochemistry 37*, 23–32.
39. Joo, C., McKinney, S. A., Lilley, D. M. J., and Ha, T. (2004) Exploring Rare Conformational Species and Ionic Effects in DNA Holliday Junctions Using Single-molecule Spectroscopy. *J. Mol. Biol. 341*, 739–751.
40. Eis, P. S., and Millar, D. P. (1993) Conformational Distributions of a Four-Way DNA junction Revealed by Time-Resolved Fluorescence Resonance Energy Transfer. *Biochemistry 32*, 13852–13860.
41. Overmas, F. J. J., and Altona, C. (1997) NMR Study of the Exchange Rate Between Two Stacked Conformers of a Model Holliday Junction. *J. Mol. Biol. 273*, 519–524.
42. Miick, S. M., Fee, R. S., Millar, D. P., and Chazin, W. J. (1997) Crossover isomer bias is the primary sequence-dependent property of immobilized Holliday junctions. *Proc. Natl. Acad. Sci. U.S.A. 94*, 9080–9084.
43. Watson, J., Hays, F. A., and Ho, P. S. (2004) Definitions and analysis of DNA Holliday junction geometry. *Nucleic Acids Res. 32*, 3017–3027.
44. Clegg, R. M., Murchie, A. I., Zechel, A., Carlberg, C., Diekmann, S., and Lilley, D. M. (1992) Fluorescence resonance energy transfer analysis of the structure of the four-way DNA junction. *Biochemistry 31*, 4846–4856.
45. Khuu, P., and Ho, P. S. (2009) A rare nucleotide base tautomer in the structure of an asymmetric DNA junction. *Biochemistry 48*, 7824–7832.
46. Clegg, R. M. (1992) Fluorescence Resonance Energy Transfer and Nucleic Acids. *Methods Enzymol. 211*, 353–388.
47. Selvin, P. R. (1995) Fluorescence Resonance Energy Transfer. *Methods Enzymol. 246*, 300–334.
48. Hillisch, A., Lorenz, M., and Diekmann, S. (2001) Recent advances in FRET: Distance determination in protein-DNA complexes. *Curr. Opin. Struct. Biol. 11*, 201–207.
49. Clegg, R. M., Murchie, A. I. H., Zechel, A., and Lilley, D. M. J. (1993) Observing helical geometry of double-stranded DNA in solution by fluorescence resonance energy transfer. *Proc. Natl. Acad. Sci. U.S.A. 90*, 2994–2998.
50. Lorenz, M., and Diekmann, S. (2006) Distance determination in protein-DNA complexes using fluorescence resonance energy transfer. *Methods Mol. Biol. 335*, 243–255.
51. Wojtuszewski, K., and Mukerji, I. (2003) HU binding to bent DNA: A fluorescence resonance energy transfer and anisotropy study. *Biochemistry 42*, 3096–3104.
52. Lorenz, M., Hillisch, A., Goodman, S. D., and Diekmann, S. (1999) Global structure similarities of intact and nicked DNA complexed with IHF measured in solution by fluorescence resonance energy transfer. *Nucleic Acids Res. 27*, 4619–4625.
53. Rice, P. A., Yang, S.-W., Mizuuchi, K., and Nash, H. A. (1996) Crystal Structure of an IHF-DNA Complex: A Protein-Induced DNA U-Turn. *Cell 87*, 1295–1306.
54. Swinger, K. K., Lemberg, K. M., Zhang, Y., and Rice, P. A. (2003) Flexible DNA bending in HU-DNA cocrystal structures. *EMBO J. 22*, 3749–3760.
55. Sagi, D., Friedman, N., Vorgias, C., Oppenheim, A. B., and Stavans, J. (2004) Modulation of DNA conformations through the formation of alternative high-order HU-DNA complexes. *J. Mol. Biol. 341*, 419–428.
56. Wojtuszewski, K., Hawkins, M. E., Cole, J. L., and Mukerji, I. (2001) HU binding to DNA: Evidence for multiple complex formation and DNA bending. *Biochemistry 40*, 2588–2598.
57. Haughland, R. P. (1996) Handbook of Fluorescent Probes and Research Chemicals, 7th ed., Molecular Probes, Inc., Eugene, OR.
58. Crosby, G. A., and Demas, J. N. (1971) The Measurement of Photoluminescence Quantum Yields. A Review. *J. Phys. Chem. 75*, 991–1024.
59. Iqbal, A., Wang, L., Thompson, K. C., Lilley, D. M., and Norman, D. G. (2008) The structure of cyanine 5 terminally attached to double-stranded DNA: Implications for FRET studies. *Biochemistry 47*, 7857–7862.
60. Lakowicz, J. R. (1999) Principles of Fluorescence Spectroscopy, 2nd ed., Kluwer Academic/Plenum, New York.
61. Lorenz, M., and Diekmann, S. (2001) Quantitative distance information on protein-DNA complexes determined in polyacrylamide gels by fluorescence resonance energy transfer. *Electrophoresis 22*, 990–998.
62. Lilley, D. M. J. (2000) Structures of helical junctions in nucleic acids. *Q. Rev. Biophys. 33*, 109–159.
63. Vamosi, G., Gohlke, C., and Clegg, R. M. (1996) Fluorescence characteristics of 5-carboxytetramethylrhodamine linked covalently to the 5′ end of oligonucleotides: Multiple conformers of single-stranded and double-stranded dye-DNA complexes. *Biophys. J. 71*, 972–994.
64. Karymov, M., Daniel, D., Sankey, O. F., and Lyubchenko, Y. L. (2005) Holliday junction dynamics and branch migration: Single-molecule analysis. *Proc. Natl. Acad. Sci. U.S.A. 102*, 8186–8191.
65. Eichman, B. F., Vargason, J. M., Mooers, B. M. H., and Ho, P. S. (2000) The Holliday junction in an inverted repeat sequence: Sequence effects on the structure of the four-way junctions. *Proc. Natl. Acad. Sci. U.S.A. 97*, 3971–3976.
66. Hays, A. F., Watson, J., and Ho, P. S. (2003) Caution! DNA Crossing: Crystal Structures of Holliday Junctions. *J. Biol. Chem. 278*, 49663–49666.

67. Thorpe, J. H., Gale, B. C., Teixeira, S. C. M., and Cardin, C. J. (2003) Conformational and Hydration Effects of Site-selective Sodium, Calcium and Strontium Ion Binding to the DNA Holliday Junction Structure d(TCGGTACCGA)$_4$. *J. Mol. Biol. 327*, 97–109.
68. Mollegaard, N. E., Murchie, A. I. H., Lilley, D. M. J., and Nielsen, P. (1994) Uranyl photoprobing of a four-way DNA junction: Evidence for specific metal ion binding. *EMBO J. 13*, 1508–1513.
69. Ohtaki, H., and Radnai, T. (1993) Structure and Dynamics of Hydrated Ions. *Chem. Rev. 93*, 1157–1204.
70. Biertümpfel, C., Yang, W., and Suck, D. (2007) Crystal structure of T4 endonuclease VII resolving a Holliday junction. *Nature 449*, 616–620.
71. Naseem, R., and Webb, M. (2008) Analysis of the DNA binding activity of BRCA1 and its modulation by the tumour suppressor p53. *PLoS One 3*, e2336.
72. Toth, K., Sauermann, V., and Langowski, J. (1998) DNA Curvature in Solution Measured by Fluroescence Resonance Energy Transfer. *Biochemistry 37*, 8173–8179.